Atomic and electronic structures in liquid arsenic telluride by *ab initio* molecular dynamics simulations

2002 J. Phys.: Condens. Matter 14 8425

(http://iopscience.iop.org/0953-8984/14/36/302)

INSTITUTE OF PHYSICS PUBLISHING JOURNAL OF PHYSICS: CONDENSED MATTER

J. Phys.: Condens. Matter **14** (2002) 8425–8433 PII: S0953-8984(02)32956-4

Atomic and electronic structures in liquid arsenic telluride by *ab initio* molecular dynamics simulations

Fuyuki Shimojo[1], **Kozo Hoshino**[1] **and Y Zempo**[2]

[1] Faculty of Integrated Arts and Sciences, Hiroshima University, Higashi-Hiroshima 739-8521, Japan
[2] Sumitomo Chemical, 6 Kitahara, Tsukuba 300-3294, Japan

E-mail: shimojo@minerva.ias.hiroshima-u.ac.jp

Received 23 January 2002, in final form 13 May 2002
Published 29 August 2002
Online at stacks.iop.org/JPhysCM/14/8425

Abstract

The temperature dependence of atomic and electronic structures in the liquid As_2Te_3 is studied by means of *ab initio* molecular dynamics simulations. The microscopic mechanism of the semiconductor–metal transition in this liquid mixture with increasing temperature and pressure is discussed compared with that in the liquid As_2Se_3. It is shown that the structure of the liquid As_2Te_3 does not change qualitatively with increasing temperature in the sense that most of the As and Te atoms continue to have three- and twofold coordination, respectively, which is contrast with the structural change from the network structure to the chain-like structure seen in the liquid As_2Se_3 at high temperatures. It is clarified that the electronic states around Te atoms contribute importantly to the metallization.

1. Introduction

The solid Te has a trigonal structure which consists of infinite twofold-coordinated helical chains of covalently bonded atoms and has semiconducting properties. On melting, the electrical conductivity increases to about 2000 Ω^{-1} cm^{-1} and the liquid Te exhibits metallic properties. The diffraction measurements [1–3] have suggested that there exists a high density of threefold-coordinated defects in the chain structure, which are considered to be responsible for the metallic conduction in the liquid phase. By adding alkali elements to the liquid Te, the electrical conductivity decreases monotonically to only about 1 Ω^{-1} cm^{-1} at 50% of alkali concentration [4–6]. Both experimental [7, 8] and theoretical [9, 10] studies have suggested that the decrease in electrical conductivity is due to the fact that the Te chains are stabilized by adding alkali elements so as to reduce the number of threefold-bonded defects. These features are quite peculiar to Te compared with those of other liquid chalcogens, S and Se, which show semiconducting properties and have a clear twofold-coordinated ring/chain structure in both solid and liquid phases.

The chalcogen atoms form stoichiometric compounds with As atoms such as As_2Se_3 and As_2Te_3. While the electronic structure in the liquid phases of these mixtures is semiconducting in character near the triple point, they exhibit metallic properties with increasing temperature and pressure [11–14]. The electrical conductivity measurements [11, 12] showed that in the liquid As_2Te_3 the semiconductor–metal (SCM) transition occurs just above the melting point. The liquid As_2Se_3 has metallic properties above 1000 °C, at which point the optical gap vanishes [13].

The liquid As_2Se_3 has a three-dimensional network structure [15]; the As and Se atoms have basically three- and twofold coordinations, respectively, and the hetero-coordination is preferred. The semiconducting properties near the triple point are due to the preservation of a covalent bonding [11]. X-ray diffraction [16] and extended x-ray absorption fine structure (EXAFS) [17] measurements were carried out for a wide range of temperatures and pressures, and it was suggested that the local environment around the As atom changes substantially and As–As covalent bonds are formed accompanied by the SCM transition. Recently, the microscopic mechanism of metallization in the liquid As_2Se_3 was investigated by *ab initio* molecular dynamics (MD) simulations [18, 19]. It has been found that, with increasing temperature, twofold-coordinated As atoms increase, and p-like non-bonding states that are almost half-filled are generated around the twofold-coordinated As atoms, which causes the metallic state.

In contrast to the liquid As_2Se_3, the metallization of the liquid As_2Te_3 has not yet been investigated theoretically, and is not well understood, although several experimental investigations were carried out. The structural change accompanied by metallization in the liquid As_2Te_3 has been extensively studied by Endo and his collaborators using EXAFS [20–22] and neutron diffraction [23] measurements. They have investigated the bond length between atoms and the coordination number for each atom as a function of temperature. Uemura *et al* [24] also investigated the structure of the liquid As_2Te_3 by neutron diffraction.

While the solid As_2Se_3 has the layer structure (monoclinic, space group $P2_1/n$), in which each As atom is surrounded by three Se atoms, and each Se atom is surrounded by two As atoms, the solid As_2Te_3 has a rather complicated structure (monoclinic, space group $C2/m$), where Te atoms have threefold coordination and As atoms have six- or sevenfold coordination with various bond distances. It is, therefore, worthwhile investigating structural differences in the liquid states of these mixtures. Also it is interesting to see if the peculiar features of liquid Te are related to the metallization of its mixture.

In this paper, we investigate the structural and electronic properties of liquid As_2Te_3 by *ab initio* MD simulations. We discuss the microscopic mechanism of the SCM transition in this liquid mixture compared with that in the liquid As_2Se_3. In section 2, the method of *ab initio* MD simulations used here is briefly described. The results of our simulations and discussions are given in section 3. Finally we summarize our work in section 4.

2. Method of calculation

Our calculations were performed within the framework of density functional theory, in which the generalized gradient approximation [25] was used for the exchange–correlation energy. The energy functional was minimized using an iterative scheme based on the preconditioned conjugate-gradient method [26, 27]. We used the ultrasoft pseudopotential [28]. The electronic wavefunctions and the charge density were expanded in plane waves with cutoff energies of 10 and 50 Ryd, respectively, which are chosen so as to give a good convergence of the total energy. The Γ point was used for the Brillouin zone sampling. The cubic supercell contains 80 atoms, (32As + 48Te). The simulations were carried out for four thermodynamic states; the

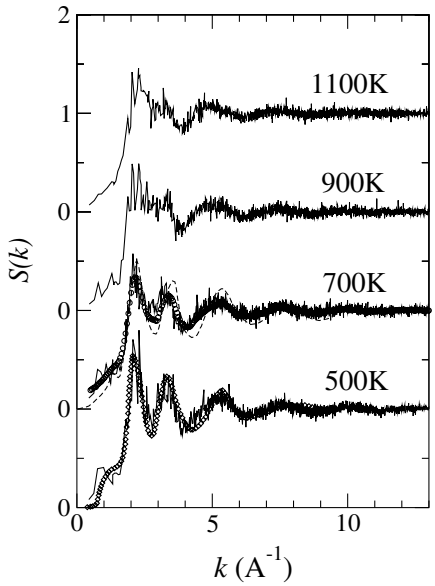

Figure 1. The temperature dependence of the total structure factor $S(k)$ of the liquid As_2Te_3. The full curves show the calculated $S(k)$. The open diamonds, open circles and broken curve show the experimental $S(k)$ measured from the x-ray diffraction for the $As_{45}Te_{55}$ glass [31], the neutron diffraction for the liquid As_3Te_7 [23] and the neutron diffraction for the liquid As_2Te_3 [24], respectively.

temperatures and densities are (500 K, 0.0302 Å^{-3}), (700 K, 0.0302 Å^{-3}), (900 K, 0.0307 Å^{-3}) and (1100 K, 0.0305 Å^{-3}), which are taken from experiments [29]. Using the Nosé–Hoover thermostat technique [30], the equations of motion were solved via the velocity Verlet algorithm with a time step $\Delta t = 2.6$–3.6 fs. Stating from the solid-state structure, we carried out the MD simulation at 2000 K for about 3 ps so that the effects of the initial configuration are ignored. The temperature of the system was gradually lowered to 1100 K at a rate of 200 K ps^{-1}. The quantities of interest were obtained by averaging over 8–10 ps after the initial equilibration, taking at least 3 ps. At all temperatures, the mean square displacements have finite slopes, which means that our system is in the liquid phase. The system at 500 K can be considered as a supercooled liquid, since the experimental melting temperature is 654 K.

3. Results and discussion

3.1. Structure factors

In figure 1, we show the calculated total structure factors, $S(k)$, by full lines for the liquids As_2Te_3, which were calculated from the partial structure factors, $S_{\alpha\beta}(k)$, with α, β = As or Te, using neutron scattering lengths. In the figure, the open diamonds, open circles and broken line show the experimental $S(k)$ measured from x-ray diffraction for the $As_{45}Te_{55}$ glass by Cornet and Rossier [31], neutron diffraction for the liquid As_3Te_7 by Maruyama *et al* [23] and neutron diffraction for the liquid As_2Te_3 by Uemura *et al* [24], respectively. We can see from this figure that the agreement between the calculations and experiments by Cornet and Rossier [31] and Maruyama *et al* [23] is very good, although the concentration used in this study is slightly different from those in the experiments. The experimental results by Uemura

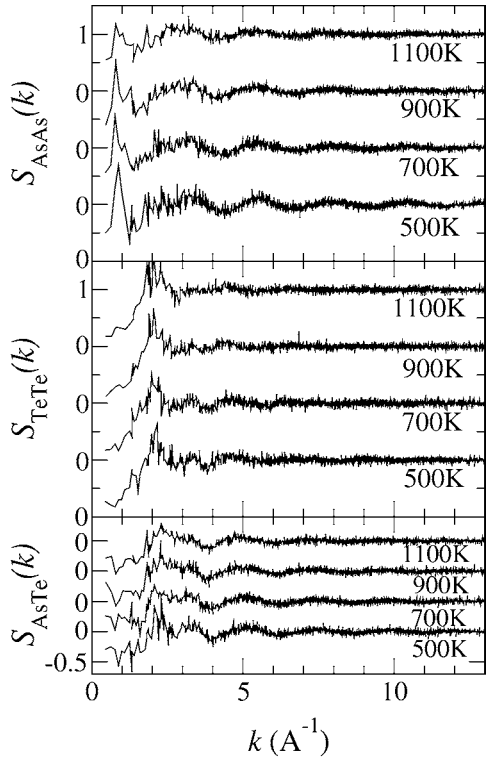

Figure 2. The temperature dependence of the partial structure factors $S_{\alpha\beta}(k)$ of the liquid As_2Te_3.

et al, however, are rather different from other experiments as well as from our results, in the sense that the positions of the first and second peaks are at higher k and the amplitude of oscillation is larger. Since the very recent experimental studies by Maruyama *et al* [23] on the structure of the liquid As_xTe_{1-x} for $x \leqslant 0.3$ show that the $S(k)$ has a weak composition dependence, we expect that the $S(k)$ for $x = 0.4$ is similar to those measured by Maruyama *et al* [23] as shown in figure 1. It is desired that further experimental investigations on the structure of the liquid As_2Te_3 are carried out.

The features observed in the calculated $S(k)$ are as follows. When the temperature is lower, there is a minimum at about $k = 2.7$ Å^{-1}, and two clear peaks can be seen at about $k = 2.0$ and 3.2 Å^{-1}. With increasing temperature, the minimum disappears gradually and the peak at about $k = 3.2$ Å^{-1} becomes a shoulder. In the smaller k (<1.5 Å^{-1}) region, the $S(k)$ does not fall smoothly to low values but has some structure.

Figure 2 shows the temperature dependence of the $S_{\alpha\beta}(k)$. It is seen that the peaks of the $S(k)$ at about $k = 2.0$ and 3.2 Å^{-1} originate mainly from peaks of the $S_{TeTe}(k)$ and $S_{AsAs}(k)$, respectively.

3.2. Pair distribution functions

Figure 3(a) shows the partial pair distribution functions, $g_{\alpha\beta}(r)$, of the liquid As_2Te_3. The temperature dependence of the first-peak positions $r_{\alpha\beta}$ of $g_{\alpha\beta}(r)$ and the coordination numbers $N_{\alpha\beta}$ are shown in figures 3(b) and (c), respectively. $N_{\alpha\beta}$ is the average number of nearest-neighbour β-type atoms around an α-type atom and is calculated as $2\rho_\beta \int_0^{r_{\alpha\beta}} 4\pi r^2 g_{\alpha\beta}(r)\,\mathrm{d}r$

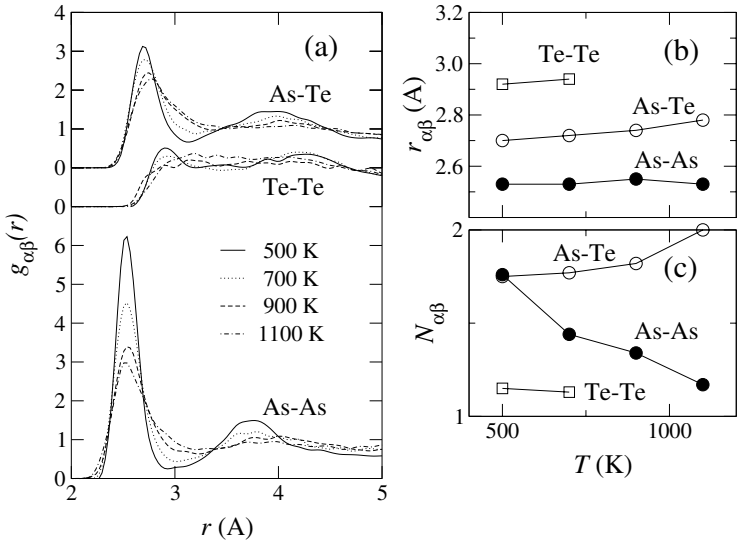

Figure 3. The temperature dependence of (a) the partial pair distribution functions $g_{\alpha\beta}(r)$, (b) the first-peak positions $r_{\alpha\beta}$ of $g_{\alpha\beta}(r)$ and (c) the coordination numbers $N_{\alpha\beta}$ for the α-type atom in the liquid As_2Te_3.

with ρ_β being the number density of β-type atoms. Since $g_{\mathrm{TeTe}}(r)$ becomes very broad with increasing temperature, r_{TeTe} and N_{TeTe} are given for only the lower two temperatures.

The remarkable features in $g_{\alpha\beta}(r)$ of the liquid As_2Te_3 are that the coordination number N_{AsAs} is the largest among the $N_{\alpha\beta}$ at 500 K and decreases with increasing temperature, as shown in figure 3(c), while N_{AsTe} increases slightly. These temperature changes in $N_{\alpha\beta}$ are quite in contrast to those in the liquid As_2Se_3 [18, 19], where N_{AsSe} has the largest value at all temperatures, which means that the neighbours around each atom are mainly unlike atoms, and N_{AsAs} and N_{SeSe} increase with increasing temperature, while N_{AsSe} decreases.

As shown in figure 3(b), the first-peak positions depend weakly on the temperature; r_{AsAs} is almost unchanged with increasing temperature, while r_{AsTe} shifts slightly to larger r. From the temperature dependence of $N_{\alpha\beta}$, we see that the coordination number for As atoms decreases with increasing temperature. These features are consistent with EXAFS measurements [20–22] in the sense that the weak temperature dependence of the first-peak positions and the temperature variation of the coordination numbers are reproduced.

3.3. Electronic density of states

The total electronic densities of states (DOS), $D(E)$, and the partial DOS [18] for α-type atoms, $D_\alpha(E)$, are shown in figure 4, where the DOSs for the liquid As_2Se_3 [18, 19] are also displayed for comparison. The origin of the energy is taken to be the Fermi level ($E_{\mathrm{F}} = 0$). In the figure, the DOSs for the electronic states above -6 eV, which are p-like in character[3], are displayed. The full curves show the $D(E)$. The full and open circles show the DOSs for As and chalcogen atoms, respectively.

As shown in figure 4(a), there are two peaks in $D_{\mathrm{Te}}(E)$ below E_{F} when the temperature is lower; one is a broad peak at around -3.5 eV and the other is a clear peak at -1 eV, which

[3] To characterize the DOS, we have calculated the angular momentum dependence of the DOS by projecting the wavefunctions on the spherical harmonics centred at all atoms.

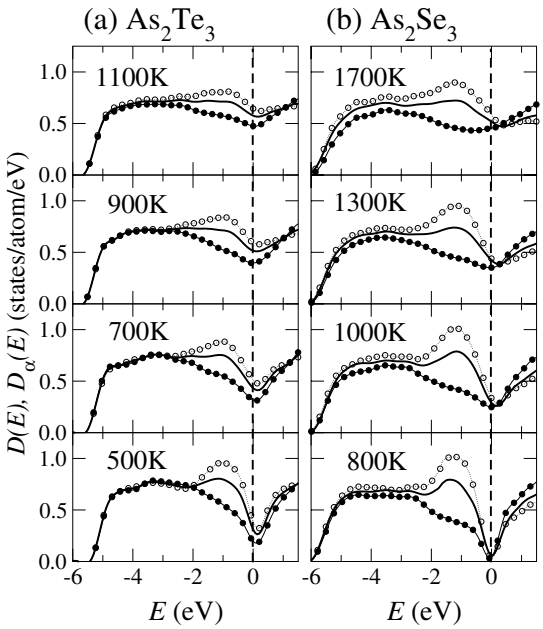

Figure 4. The temperature dependence of the electronic density of states (DOS) of the liquids (a) As_2Te_3 and (b) As_2Se_3. The full curves show the total DOS $D(E)$. The full and open circles show the partial DOS $D_\alpha(E)$ for As and chalcogen atoms, respectively. The origin of the energy is taken to be the Fermi level ($E_F = 0$).

correspond to p-like bonding and non-bonding states, respectively. At higher temperatures, these two peaks become unclear and $D_{Te}(E)$ has a very flat distribution in a wide range of energies. $D_{As}(E)$ consists of a broad peak for $E < E_F$, which is mainly contributed by the threefold-coordinated bonding states. This behaviour is very similar to that in the partial DOS in the liquid As_2Se_3 [18, 19] (see figure 4(b)).

The total $D(E)$ of the liquid As_2Te_3 has a large dip at E_F when the temperature is lower, which means that this liquid mixture has semiconducting properties. With increasing temperature, the dip is gradually filled up, which shows that the system has metallic properties. This temperature dependence of $D(E)$ is quite consistent with the conductivity measurements [11, 12]. Accompanied with filling up the dip in $D(E)$, the values of $D_{As}(E)$ and $D_{Te}(E)$ at E_F increase. The dip positions in the partial DOSs are at E_F at all temperatures. It should be noted that, in the metallic states, $D_{Te}(E)$ has a larger value than $D_{As}(E)$ at E_F.

In the case of the metallic state of the liquid As_2Se_3, the partial DOSs for As and Se atoms have almost the same value at E_F, and the dips of the partial DOSs for As and Se atoms are located at lower and higher energies relative to E_F, respectively. This indicates that some of the electrons, which occupy the p-like non-bonding states around Se atoms, will transfer to As atoms. On the other hand, it is expected that the charge transfer is very small in the liquid As_2Te_3, because there is no dip shift in the partial DOS.

3.4. Coordination number distribution functions

To see more clearly how the structural change occurs in the liquid As_2Te_3, we obtained the coordination number (n) distribution function, $P_\alpha(n)$, which is defined as the probability of

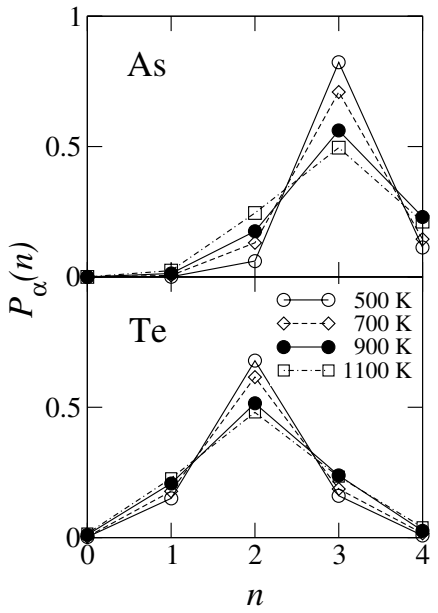

Figure 5. The temperature dependence of the coordination number (n) distribution functions $P_\alpha(n)$ of the liquid As_2Te_3.

finding n atoms around an α-type atom. We calculated $P_\alpha(n)$ simply by counting the number of atoms inside a sphere of radius R centred at each α-type atom. Figure 5 displays $P_\alpha(n)$ calculated with $R = 2.8$, 3.0, and 3.1 Å for As–As, As–Te and Te–Te pairs, respectively, which are estimated from the first-minimum positions in $g_{\alpha\beta}(r)$. Although $P_\alpha(n)$ depends somewhat on the value of R, the following qualitative features remain the same.

When the temperature is low, $P_{As}(n)$ and $P_{Te}(n)$ have large peaks at $n = 3$ and 2, respectively, which means that this liquid mixture has the three-dimensional network structure. With increasing temperature, not only $P_{As}(2)$ but also $P_{As}(4)$ increase, while $P_{As}(3)$ decreases. In the distribution of $P_{Te}(n)$, we can see a similar temperature dependence to that in $P_{As}(n)$; $P_{Te}(1)$ and $P_{Te}(3)$ increase, while $P_{Te}(2)$ decreases, when the temperature becomes higher.

In the liquid As_2Se_3 [18, 19], the temperature dependence of $P_\alpha(n)$ is different from those in the liquid As_2Te_3; more twofold-coordinated As atoms exist than threefold-coordinated ones at higher temperatures, and twofold- and onefold-coordinated Se atoms decrease and increase, respectively, with increasing temperature. This temperature dependence in $P_\alpha(n)$ clearly shows that the major part of the liquid As_2Se_3 consists of twofold chain-like structures at higher temperatures. In contrast to this structural change in the liquid As_2Se_3, there is no clear tendency of the transformation from the three-dimensional network structure to the chain-like structure in the liquid As_2Te_3. Although the threefold-coordinated As and twofold-coordinated Te decrease with increasing temperature, they have peaks in the distribution functions at all temperatures, as shown in figure 5. From these facts, we conclude that the structure of the liquid As_2Te_3 does not change qualitatively but changes quantitatively with increasing temperature.

This was confirmed by viewing directly the atomic configuration obtained by our *ab initio* MD simulation. Figures 6(a) and (b) show the snapshots of atomic configurations for two temperatures, 700 and 1100 K, respectively. The red and green balls show the positions of As and Te atoms, respectively, in the supercell. Two atoms, whose distance apart is smaller than

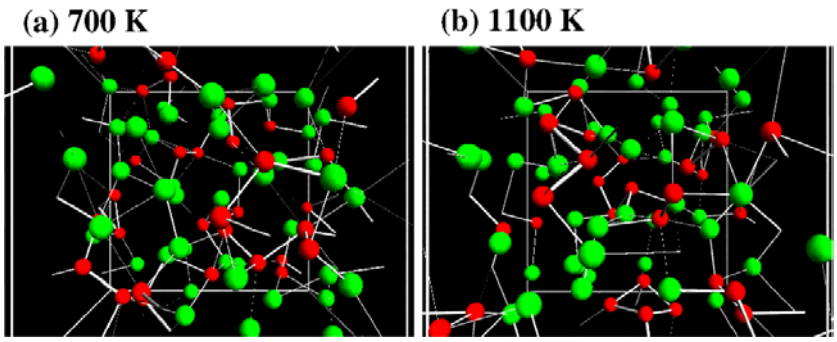

Figure 6. The atomic configurations of the liquid As_2Te_3 for two temperatures: (a) 700 K and (b) 1100 K. The red and green balls show the positions of As and Te atoms, respectively, in the supercell. Two atoms, whose distance apart is smaller than 2.8 Å, are connected by the bond.

2.8 Å, are connected by the bond. We can see that there is no clear structural change in the three-dimensional network structure.

3.5. Semiconductor–metal transition

In the case of the liquid As_2Se_3 [18, 19], the structure clearly transforms into a chain structure with increasing temperature. The twofold-coordinated As atoms in the chain-like structure should have almost the same electronic states as those of the chalcogen atoms, i.e. twofold-coordinated p-like bonding and p-like non-bonding states. To occupy these states, four p electrons per atom are needed, as is the case for the Se atom. However, since the number of p electrons in the As atom is three, the p-like non-bonding states around the twofold-coordinated As atoms will not be occupied completely, which causes the metallic behaviour and charge transfer from the Se to As atoms. In addition to this mechanism of metallization, near the Fermi level there are electronic states, whose electronic wavefunctions have a large amplitude around the onefold-coordinated atoms in the chain structure. These states are the same as those observed in the liquid Se [32]. These facts show that the electronic states around lower-coordinated atoms are important for the metallization in the liquid As_2Se_3.

On the other hand, our simulations for the liquid As_2Te_3 show that the atomic structure does not transform into a chain-like structure but into some disordered structure, where the numbers of fourfold-coordinated As and threefold-coordinated Te are comparable to those of twofold-coordinated As and onefold-coordinated Te, which indicates that this liquid mixture metallizes in a different way. The temperature dependence of the partial DOS, as shown in figure 4, demonstrates that $D_{\mathrm{Te}}(E)$ has a larger value than $D_{\mathrm{As}}(E)$ at E_{F} with increasing temperature in the liquid As_2Te_3, while two partial DOSs in the liquid As_2Se_3 have almost the same values at E_{F}. It is therefore concluded that the electronic states around Te atoms are more important for the metallization than those around As atoms in the liquid As_2Te_3, which should be compared with the metallic states in liquid Te.

4. Summary

The temperature dependence of structural and electronic properties in the liquid As_2Te_3 mixture has been investigated by means of *ab initio* MD simulations. We have mainly discussed the microscopic mechanism of the SCM transition in this liquid mixture with increasing

temperature and pressure compared with that in the liquid As_2Se_3. It is shown that the structure of the liquid As_2Te_3 does not change qualitatively with increasing temperature; the As and Te atoms have mainly three- and twofold coordination, respectively, although the number of them decrease when the temperature becomes higher. This contrasts with the fact that the network structure is transformed into a twofold chain-like structure at higher temperatures in the liquid As_2Se_3. It is clarified that the electronic states around Te atoms contribute importantly to the metallization in the liquid As_2Te_3, while the electronic states around lower-coordinated As as well as Se atoms are essential for the metallization in the liquid As_2Se_3.

Acknowledgments

We acknowledge Professor K Maruyama, Professor H Hoshino and Professor H Endo for useful discussions and for providing us with their experimental data. We also thank Professor K Tamura for useful discussions and encouragement. This work was supported by a Grant-in-Aid for Scientific Research from The Ministry of Education, Science, Sports and Culture, Japan. We are grateful to the Supercomputer Center, Institute for Solid State Physics, University of Tokyo for the use of Hitachi SR8000 and SGI Origin 2800.

References

[1] Takeda S, Tamaki S and Waseda Y 1984 *J. Phys. Soc. Japan* **53** 3830
[2] Munelle A, Bellissent R and Frank A M 1989 *Physica* B **156–7** 174
[3] Tsuzuki T, Yao M and Endo H 1995 *J. Phys. Soc. Japan* **64** 485
[4] Kraus C A and Glass S W 1929 *J. Phys. Chem.* **33** 984
[5] Saboungi M-L, Fortner J, Richardson J W, Petric A, Doyle M and Enderby J E 1993 *J. Non-Cryst. Solids* **156–8** 356
[6] Kawakita Y, Yao M, Endo H and Dong J 1996 *J. Non-Cryst. Solids* **205–7** 447
[7] Fortner J, Saboungi M-L and Enderby J E 1992 *Phys. Rev. Lett.* **69** 1415
[8] Kawakita Y, Yao M and Endo H 1997 *J. Phys. Soc. Japan* **66** 1339
[9] Shimojo F, Hoshino K and Zempo Y 1999 *Phys. Rev.* B **59** 3514
[10] Shimojo F, Hoshino K and Zempo Y 2001 *Phys. Rev.* B **63** 094206
[11] Edmond J T 1966 *Br. J. Appl. Phys.* **17** 979
[12] Oberafo A A 1975 *J. Phys. C: Solid State Phys.* **8** 469
[13] Hosokawa S, Sakaguchi Y, Hiasa H and Tamura K 1991 *J. Phys.: Condens. Matter* **3** 6673
[14] Hoshino H, Miyanaga T, Ikemoto H, Hosokawa S and Endo H 1996 *J. Non-Cryst. Solids* **205–7** 43
[15] Uemura O, Sagara Y, Muno D and Satow T 1978 *J. Non-Cryst. Solids* **30** 155
[16] Hosokawa S, Sakaguchi Y and Tamura K 1992 *J. Non-Cryst. Solids* **150** 35
[17] Tamura K, Hosokawa S, Inui M, Yao M, Endo H and Hoshino H 1992 *J. Non-Cryst. Solids* **150** 351
[18] Shimojo F, Munejiri S, Hoshino K and Zempo Y 1999 *J. Phys.: Condens. Matter* **11** L153
[19] Shimojo F, Munejiri S, Hoshino K and Zempo Y 2000 *J. Phys.: Condens. Matter* **12** 6161
[20] Hosokawa S, Tamura K, Inui M and Endo H 1993 *J. Non-Cryst. Solids* **156–8** 712
[21] Ikemoto H, Hoshino H, Miyanaga T, Yamamoto I and Endo H 1999 *J. Non-Cryst. Solids* **250–2** 458
[22] Endo H, Hoshino H, Ikemoto H and Miyanaga T 2000 *J. Phys.: Condens. Matter* **12** 6077
[23] Maruyama K, Hoshino H, Ikemoto H, Miyanaga T and Endo H 2001 private communication
[24] Uemura O, Sagara Y, Tsushima M, Kamikawa T and Satow T 1979 *J. Non-Cryst. Solids* **33** 71
[25] Perdew J P, Burke K and Ernzerhof M 1996 *Phys. Rev. Lett.* **77** 3865
[26] Kresse G and Hafner J 1994 *Phys. Rev.* B **49** 14 251
[27] Shimojo F, Zempo Y, Hoshino K and Watabe W 1995 *Phys. Rev.* B **52** 9320
[28] Vanderbilt D 1990 *Phys. Rev.* B **41** 7892
[29] Tsuchiya Y 1999 *J. Non-Cryst. Solids* **250–2** 473
[30] Nosé S 1984 *Mol. Phys.* **52** 255
Hoover W G 1985 *Phys. Rev.* A **31** 1695
[31] Cornet J and Rossier D 1973 *J. Non-Cryst. Solids* **12** 85
[32] Shimojo F, Hoshino K, Watabe M and Zempo Y 1998 *J. Phys.: Condens. Matter* **10** 1199